

PhotoD: LSST photometric distances out to 100 kpc.

LOVRO PALAVERSA ¹, ŽELJKO IVEZIĆ ², AND KARLO MRAKOVČIĆ ³

¹*Ruder Bošković Institute, Bijenička cesta 54, 10000 Zagreb, Croatia*

²*Department of Astronomy, University of Washington, Box 351580, Seattle, WA 98195, USA*

³*Faculty of Physics, University of Rijeka, Radmile Matejčić 2, 51000 Rijeka, Croatia*

ABSTRACT

This example manuscript is intended to serve as a tutorial and template for authors to use when writing their own AAS Journal articles. The manuscript includes a history of AAST_EX and documents the new features in the previous versions as well as the bug fixes in version 6.31. This manuscript includes many figure and table examples to illustrate these new features. Information on features not explicitly mentioned in the article can be viewed in the manuscript comments or more extensive online documentation. Authors are welcome to replace the text, tables, figures, and bibliography with their own and submit the resulting manuscript to the AAS Journals peer review system. The first lesson in the tutorial is to remind authors that the AAS Journals, the Astrophysical Journal (ApJ), the Astrophysical Journal Letters (ApJL), the Astronomical Journal (AJ), and the Planetary Science Journal (PSJ) all have a 250 word limit for the abstract^a. If you exceed this length the Editorial office will ask you to shorten it. This abstract has 182 words.

Keywords: Distance measure (395) — Interstellar extinction (841) — Photometry (1234) — Stellar distance (1595) — Two-color diagrams (1724)

1. INTRODUCTION

Thanks to the *Vera C. Rubin* observatory's *Legacy Survey of Space and Time* (LSST), for the first time in history, an astronomical catalog will contain more Milky Way stars than there are living people on Earth – of the order 10-20 billion, depending on model assumptions. In order to map the Milky Way in three dimensions, distances to these stars must be accurately estimated. In this paper we describe a method that will deliver LSST-based stellar distance estimations complementary to *Gaia*'s state-of-the-art trigonometric parallaxes and reach about 10 times further, to approximately 100 kpc. These results will be transformative for the studies of the Milky Way in general, and the stellar and the dark matter halo in particular as never before was there a survey that simultaneously observed roughly two thirds of the sky, to the co-added depth of $r \approx 26$ mag.

A bit about the importance of the distance estimation in the MW, dust implications (for extragalactic science too).

There are a variety of astronomical methods to estimate distances to stars, ranging from direct geometric (trigonometric) methods for nearby stars to indirect methods based on astrophysics for more distant stars.

Mention Bailer-Jones et al. (2021), Gordon et al. (2016), Green et al. (2014, 2015, 2019), Jurić et al. (2008) and Lallement et al. (2014), Queiroz et al. (2018).

Layout of the paper is...

^a) Abstracts for Research Notes of the American Astronomical Society (RNAAS) are limited to 150 words

2. METHOD

The photometric distance estimation method (hereafter **photoD**) is conceptually quite simple and relies on the strong correlations between the stellar colors and spectral energy distributions (SED) for dominant stellar populations. The stellar spectral energy distributions, and consequently colors, are determined by the effective temperature (T_{eff}), the surface gravity (g), and the metallicity ($[M/H]$), or alternatively, by the absolute magnitude in band b (M_b), $[M/H]$ and age.

The distributions that describe these correlations are obtained either from models or from observations. For example, the distribution of stellar SEDs in the color-color diagram in Figure ?? provides key insights in stellar evolution and classification of different stellar populations such as main-sequence stars, giant stars, white dwarf stars, a majority of unresolved binary stars and even extragalactic objects. Analogous distributions are responsible for the abundant structure seen in the Hertzsprung-Russell diagram (HRD).

Metallicity is an important factor in these correlations, as it has a strong effect on the luminosity of the stars. This is reflected in the width of the main stellar loci of the color-magnitude diagrams (CMD) of the stellar populations observed at the same distance and the two-color diagrams (**quantify**), as seen in Figure ?. The best photometric estimators of metallicity are colors whose shorter-wavelength component includes the metal absorption bands at near-UV wavelengths, short of Balmer break ($300 \lesssim \lambda \text{ [nm]} \lesssim 400$). Therefore, the LSST has a comparative advantage over the surveys lacking u -band measurements, and could provide accurate distances within the range of 5-10%. **A plot of model spectra, fixed, $\log(g)$ and T_{eff} , several different metallicities?**

Extinction is another major source of systematic errors in the process of luminosity and distance determination. The fact that the extinction vector is nearly parallel to the main stellar locus in the two-color diagrams gives rise to degeneracies that complicate the determination of the stellar type. An example is displayed in Fig. ??, where in the left panel any of the different star types designated as 1,2 and 3 can have the same observed colors as the star marked as "Obs". This degeneracy is a result of the combination of colors chosen for the two-color diagram and depends on the position on the stellar locus and the adopted extinction curve parametrized by a single parameter R_V

$$R_V = \frac{A_V}{E(B-V)}, \quad (1)$$

where A_V stands for extinction in V -band and $E(B-V)$ is the color excess. This relationship can be extended to an arbitrary photometric bandpass λ :

$$A_\lambda = C_\lambda(R_V)A_r, \quad (2)$$

with A_r designating extinction in r -band and $C_\lambda(R_V)$ describing the shape of the extinction curve. The degeneracy from the left panel in Fig. ?? can be broken if several different colors are used, particularly those towards the infrared, where the stellar locus is not kinked and the extinction vector is not parallel to it (as shown in the right panel of the Figure ??), where $r-i$ and $i-z$ colors are used, and assuming a fixed extinction law a unique solution for the extinction is possible.

Explain the choice of RV .

Another important degeneracy arises from the fact that even for a fixed T_{eff} and $[Fe/H]$, the $\log(g)$ and thus the luminosity are not uniquely determined by the colors: a degeneracy may exist between the giant branch and the main sequence as the colors constructed from $ugrizy$ bands are not sensitive to $\log(g)$ (**As evident from \tilde{Z} 's gr-ri plot.**). We treat this issue by adopting a prior based on bins in apparent magnitude.

We adopt a Bayesian framework in which we simultaneously fit for M_b , $[Fe/H]$ and A_r , assuming a fixed RV value of 3.1¹ The posterior for each individual star with LSST photometry is then given as:

$$P(M_b, [Fe/H], A_r | \vec{c}) = \frac{P(\vec{c} | M_b, [Fe/H], A_r) P(M_b, [Fe/H], A_r)}{P(\vec{c})} \quad (3)$$

with \vec{c} standing for the vector of input colors ($u-g$, $g-r$ and so on). The log-likelihood is given by:

$$\ln(\mathcal{L}) = C - \frac{1}{2} \sum_{i=1}^N \left(\frac{c_i^{obs} - c_i^{mod}}{\sigma_i} \right)^2 \quad (4)$$

where c_i^{obs} are the observed colors and c_i^{mod} model colors. The values of model colors and the priors are extracted from from TRILEGAL (Dal Tio et al. (2022)). In order to extract the priors (i.e. prior maps), we divide TRILEGAL data in healpix bins, and further subdivide them in one-magnitude wide bins in apparent magnitude. The latter subdivision is helpful in breaking the degeneracies between the giant and dwarf stars, as in-

¹ In principle RV could be also fitted for.

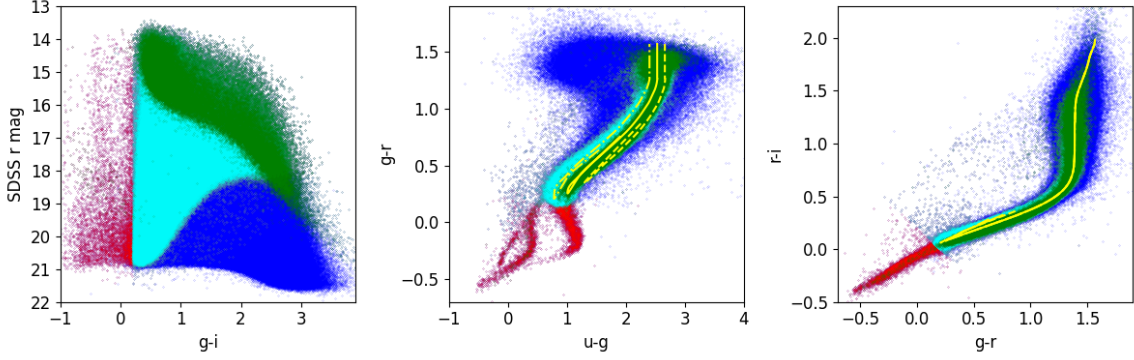


Figure 1. Copy caption from email

trinsically luminous stars become strongly disfavored at faint magnitudes².

Add plots describing the method, and go through one example like in Željko's slides.

Our method is basically brute-force fitting with some intelligent tricks leveraged to obtain faster execution that will be required for 10B LSST stars. We use Schlegel et al. (1998) (SFD98) maps in order to limit the range of the extinction. This is usually a valid assumption because the SFD98 maps provide *total* extinction along a line of sight. Our fitting procedure is also executed on an adaptive grid, a coarse search over the parameter space is performed first in order to establish the layout of the manifold. However, care is taken that any possible local minima are not missed by appropriately adjusting the step size *how?*. The located maxima are then explored with a smaller step size (*adjusted how?*).

In addition to the approach described here, we also tested Markov Chain Monte Carlo and neural network approaches that will be/are described in forthcoming/published papers.

Advantages & disadvantages of the model-based and empirical approaches, how model based approaches can be improved by adding empirical information for specific cases.

Gordon et al. (2016) na BEAST webu imaju zgodne diagrame; možda bi i mi mogli nešto tog tipa napraviti, bar za draft, primjer

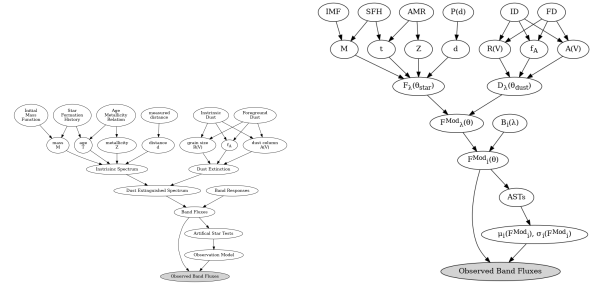


Figure 2. BEAST.

² In other words, an apparently faint giant star would imply a very large distance. For example a moderately bright giant star with $M_r=0$ mag and $r=22$ mag would imply a distance modulus of 22 mag, or distance of approximately 251 kpc.

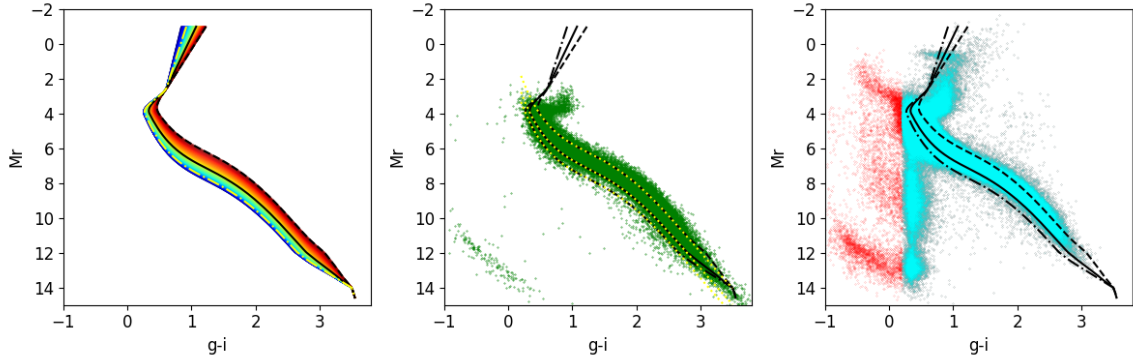


Figure 3. Copy caption from email

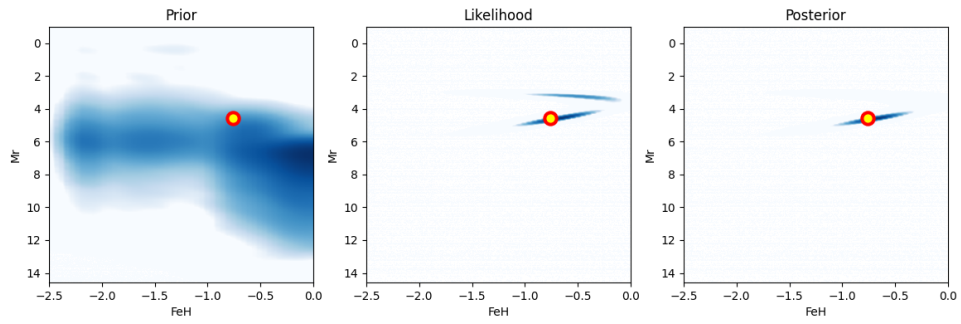


Figure 4. Write caption: prior, likelihood, posterior maps

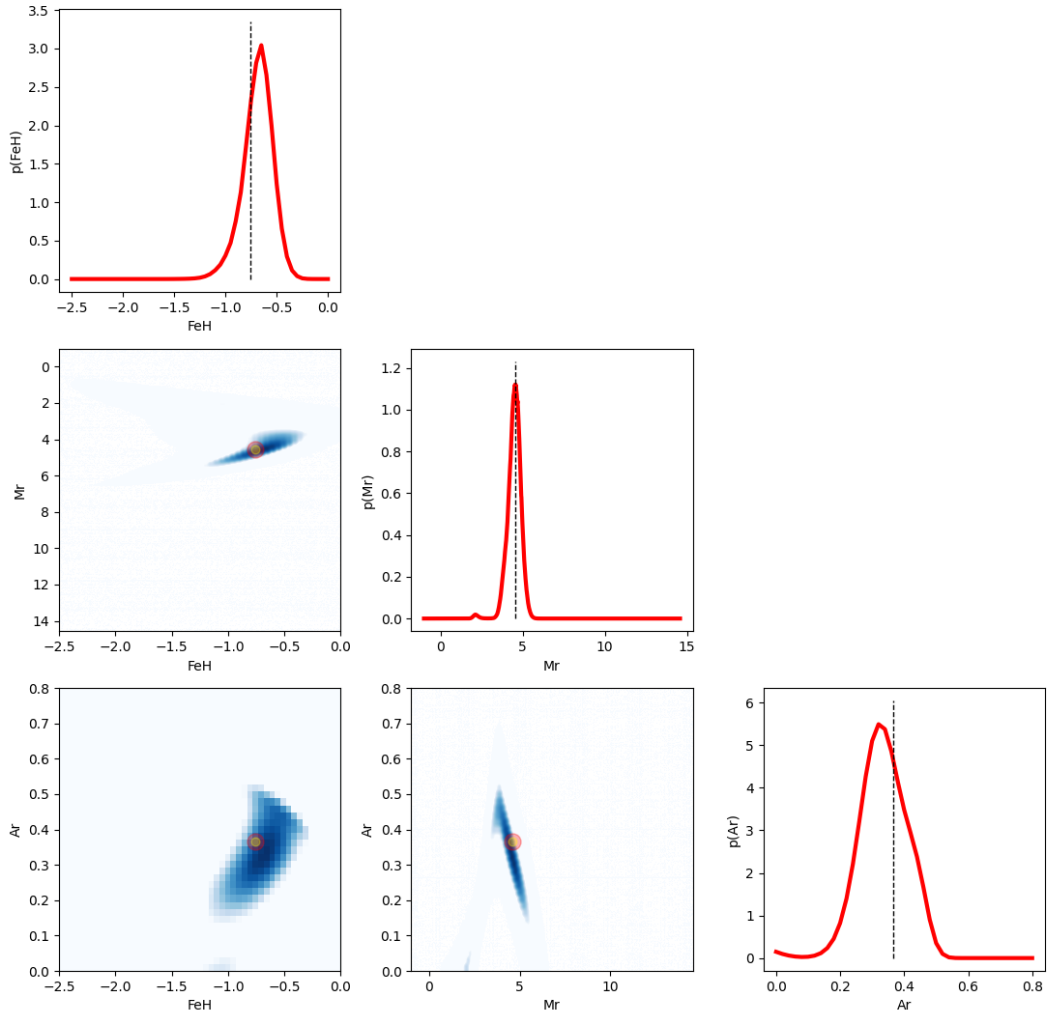


Figure 5. Write caption: 2-param covariances and marginal distributions

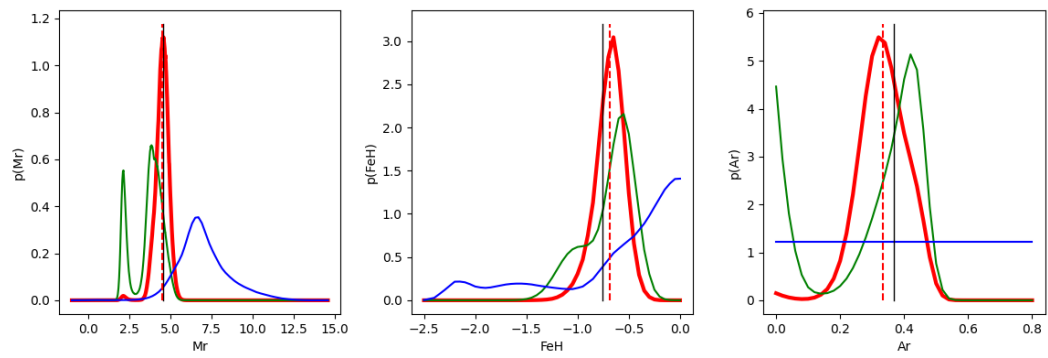


Figure 6. Write caption: prior, likelihood, posterior marginal distributions

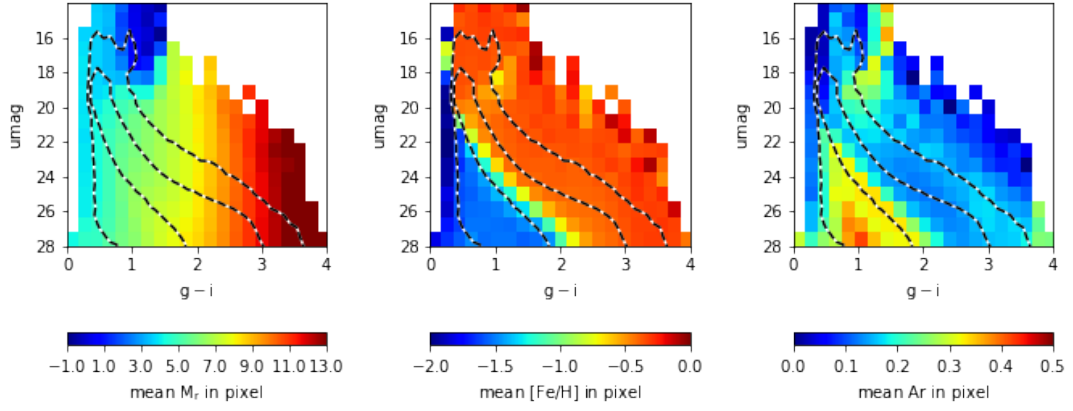


Figure 7. Write caption: TRILEGAL mean values of input model params in umag vs. g-i

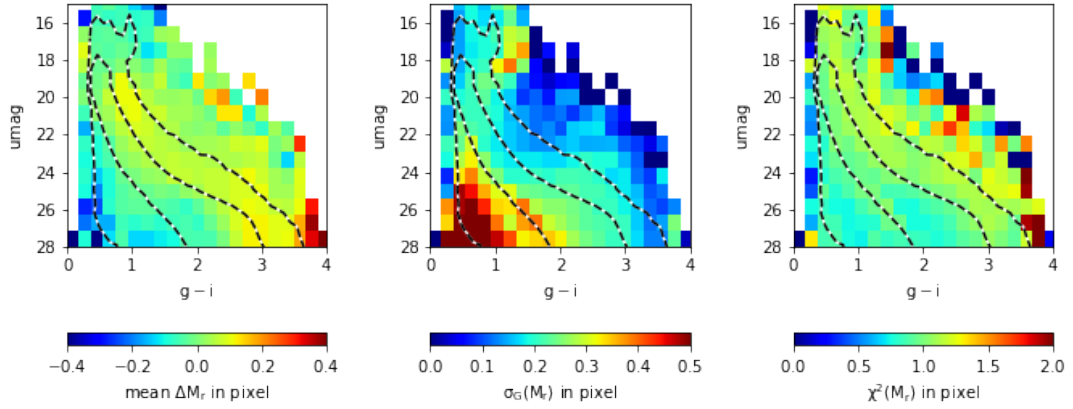


Figure 8. Write caption: performance for Mr vs. true Mr and FeH

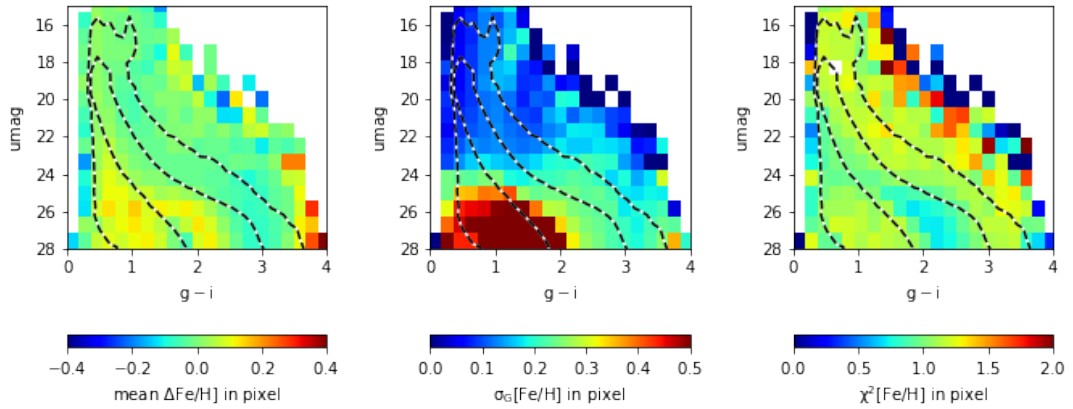


Figure 9. Write caption: performance for FeH vs. true Mr and FeH

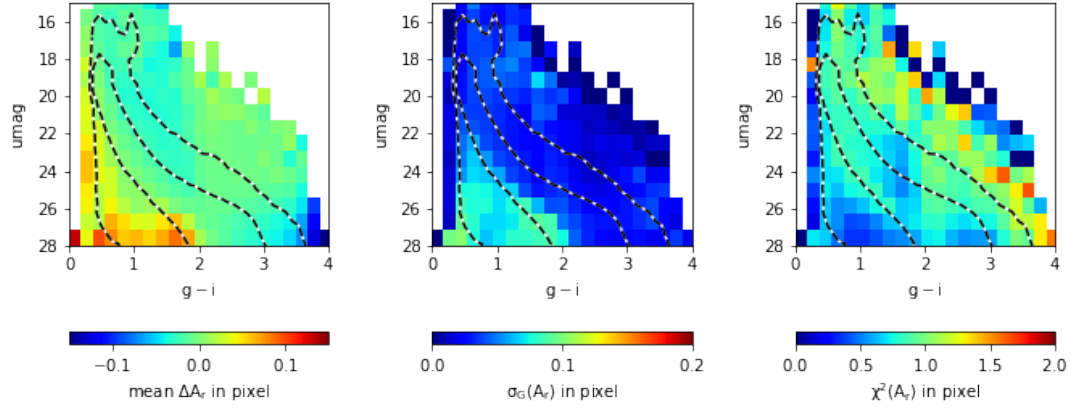


Figure 10. Write caption: performance for Ar vs. true Mr and FeH

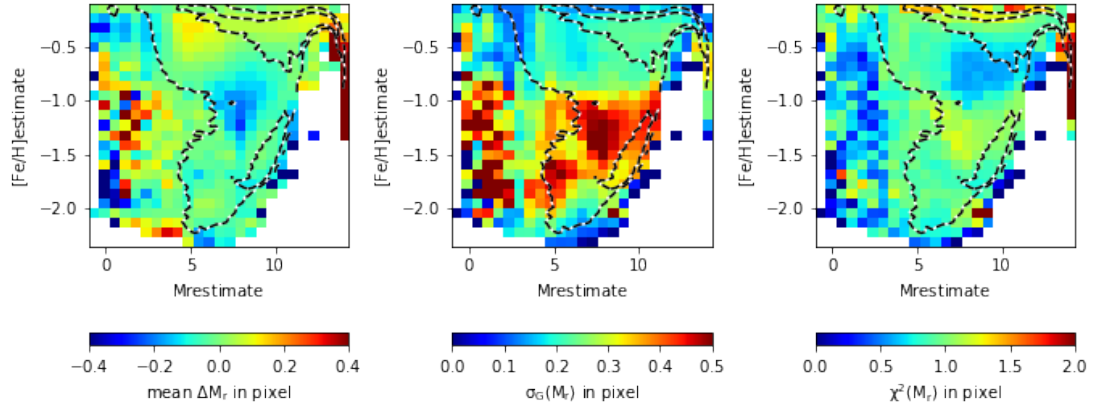


Figure 11. Write caption: performance for Mr vs. estimated Mr and FeH

APPENDIX

REFERENCES

- 164 Bailer-Jones, C. A. L., Rybizki, J., Fouesneau, M.,
 165 Demleitner, M., & Andrae, R. 2021, *AJ*, 161, 147,
 166 doi: [10.3847/1538-3881/abd806](https://doi.org/10.3847/1538-3881/abd806)
- 167 Dal Tio, P., Pastorelli, G., Mazzi, A., et al. 2022, *The*
 168 *Astrophysical Journal Supplement Series*, 262, 22,
 169 doi: [10.3847/1538-4365/ac7be6](https://doi.org/10.3847/1538-4365/ac7be6)
- 170 Gordon, K. D., Fouesneau, M., Arab, H., et al. 2016, *The*
 171 *Astrophysical Journal*, 826, 104,
 172 doi: [10.3847/0004-637X/826/2/104](https://doi.org/10.3847/0004-637X/826/2/104)
- 173 Green, G. M., Schlafly, E., Zucker, C., Speagle, J. S., &
 174 Finkbeiner, D. 2019, *The Astrophysical Journal*, 887, 93,
 175 doi: [10.3847/1538-4357/ab5362](https://doi.org/10.3847/1538-4357/ab5362)
- 176 Green, G. M., Schlafly, E. F., Finkbeiner, D. P., et al. 2014,
 177 *ApJ*, 783, 114, doi: [10.1088/0004-637X/783/2/114](https://doi.org/10.1088/0004-637X/783/2/114)
- 178 —. 2015, *ApJ*, 810, 25, doi: [10.1088/0004-637X/810/1/25](https://doi.org/10.1088/0004-637X/810/1/25)
- 179 Jurić, M., Ivezić, Ž., Brooks, A., et al. 2008, *The*
 180 *Astrophysical Journal*, 673, 864, doi: [10.1086/523619](https://doi.org/10.1086/523619)
- 181 Lallement, R., Vergely, J.-L., Valette, B., et al. 2014, *A&A*,
 182 561, A91, doi: [10.1051/0004-6361/201322032](https://doi.org/10.1051/0004-6361/201322032)
- 183 Queiroz, A. B. A., Anders, F., Santiago, B. X., et al. 2018,
 184 *Monthly Notices of the Royal Astronomical Society*, 476,
 185 2556, doi: [10.1093/mnras/sty330](https://doi.org/10.1093/mnras/sty330)
- 186 Schlegel, D. J., Finkbeiner, D. P., & Davis, M. 1998, *The*
 187 *Astrophysical Journal*, 500, 525, doi: [10.1086/305772](https://doi.org/10.1086/305772)